

HALL-PETCH HARDENING IN PULSED LASER DEPOSITED NICKEL AND COPPER THIN FILMS

J. A. KNAPP, D. M. FOLLSTAEDT, J. C. BANKS, AND S. M. MYERS
Sandia National Laboratories, Albuquerque, NM 87185-1056

RECEIVED
JAN 24 2000
OSTI

ABSTRACT

Very fine-grained Ni and Cu films were formed using pulsed laser deposition on fused silica substrates. The grain sizes in the films were characterized by electron microscopy, and the mechanical properties were determined by ultra-low load indentation, with finite-element modeling used to separate the properties of the layers from those of the substrate. Some Ni films were also examined after annealing to 350 and 450°C to enlarge the grain sizes. These preliminary results show that the observed hardnesses are consistent with a simple extension of the Hall-Petch relationship to grain sizes as small as 11 nm for Ni and 32 nm for Cu.

INTRODUCTION

The hardness and yield stress of polycrystalline materials is generally observed to increase as the grain size is decreased according to the Hall-Petch relationship [1-2]

$$H = H_0 + Kd^{-1/2} \quad (1)$$

where d is the grain diameter and H_0 and K are constants. Since the physical basis of this empirical dependence is thought to be the pileup of dislocations within grains, the relation is expected to fail at sufficiently small grain sizes, when the volume of material is too small for a dislocation model to be meaningful. Some previous experiments on both Ni and Cu appear to indicate that the relationship fails at 50-100 nm grain size [3-9], with some experiments even showing a slight softening with decreasing grain size in the range of 5-20 nm. The purpose of this work was to further explore the limits of applicability of the Hall-Petch relationship in both Ni and Cu.

The challenge in testing the limits of the Hall-Petch relationship is to produce very fine-grained material free of impurities and voids. In the present work, we used pulsed laser deposition (PLD), which produces clean, uniform layers with very fine grains at room temperature. Transmission electron microscopy (TEM) showed that the sizes in layers deposited at room temperature were ~11 nm and ~32 nm, respectively, for Ni and Cu. Ultra-low-load indentation testing combined with an analysis based on finite-element modeling was then used to evaluate the mechanical properties of the layers.

LAYER SYNTHESIS AND MICROSTRUCTURE CHARACTERIZATION

The layers were deposited in an all-metal vacuum chamber using a KrF excimer laser. The wavelength was 248 nm, with 34 ns fwhm pulse width, operated at 35 Hz. The Ni or Cu targets were rastered in x and y to use several square cm of the targets for source material during deposition. For Ni, about 0.007 nm of material was deposited with each shot, yielding a 0.25 nm/sec growth rate. The system includes an active particle filter in the form of a spinning, slotted disk between the ablation target and the deposition substrate. The laser is fired in synchronization with the disk, such that the high-energy plasma component of the ablation plume passes through

DISCLAIMER

This report was prepared as an account of work sponsored by an agency of the United States Government. Neither the United States Government nor any agency thereof, nor any of their employees, make any warranty, express or implied, or assumes any legal liability or responsibility for the accuracy, completeness, or usefulness of any information, apparatus, product, or process disclosed, or represents that its use would not infringe privately owned rights. Reference herein to any specific commercial product, process, or service by trade name, trademark, manufacturer, or otherwise does not necessarily constitute or imply its endorsement, recommendation, or favoring by the United States Government or any agency thereof. The views and opinions of authors expressed herein do not necessarily state or reflect those of the United States Government or any agency thereof.

DISCLAIMER

**Portions of this document may be illegible
in electronic image products. Images are
produced from the best available original
document.**

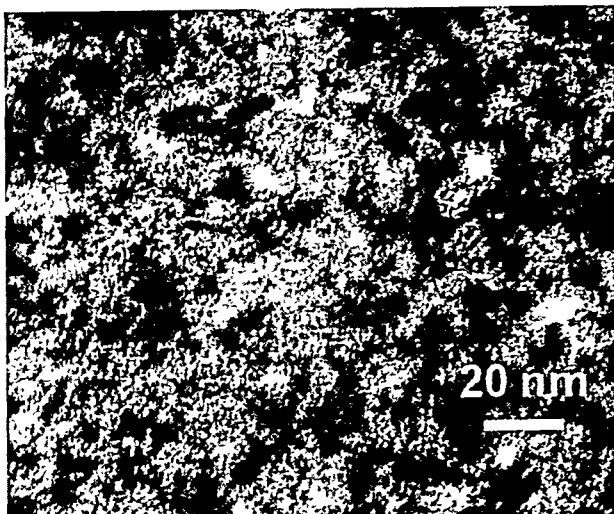


Figure 1. Bright-field TEM micrograph of as-deposited Ni film.

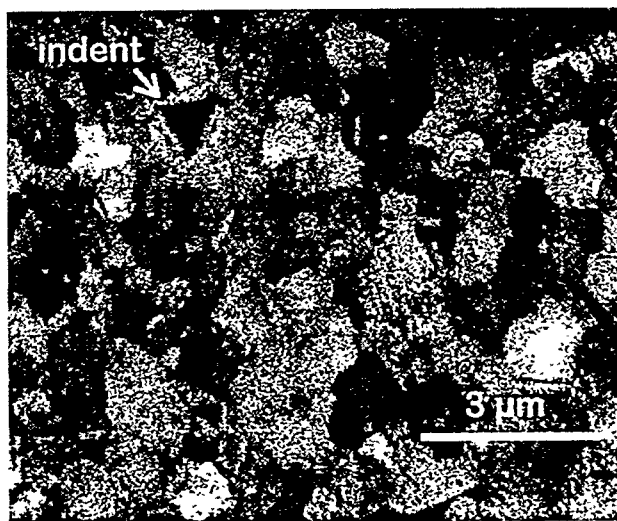


Figure 2. Backscattered electron image of Ni film after a 1 hr. anneal at 450°C. The residual impression from one of the indents used for mechanical property measurements is also shown.

the slot to be quenched on the substrate, but slower droplets and other particles are largely blocked. Chamber pressure during depositions was typically 2×10^{-7} Torr. Films were deposited on fused silica substrates to a thickness of 700-800 nm. Thinner films were also deposited on coated TEM disks for direct examination in an electron microscope.

After deposition the film areal atomic density and purity were characterized by Rutherford backscattering spectrometry, showing O at less than ~5 at.%. The film thickness was measured by a profilometer. The as-deposited material was characterized by using a TEM to examine the thin films on grids in plan view. Figure 1 shows a typical bright-field TEM image from an as-deposited Ni film, obtained using 200 keV. The material is crystalline with highly disordered grain boundaries. Diffraction from the layer shows little or no evidence for any amorphous areas, as would be expected, since pure metals are very difficult to amorphize. Measurements using this micrograph as well as others gave an average grain size of 11.2 nm with a standard deviation of 3.1 nm. Similar examination of as-deposited Cu films (not shown) showed a similar microstructure with an average grain size of 32 nm and a standard deviation of 10 nm.

For Ni, two of the as-deposited films were annealed in order to increase the grain size and thereby measure the hardness at larger sizes. These anneals were performed both *in situ* for the thin films in the TEM and in a vacuum furnace for the thicker layers on silica. Grain sizes for the *in situ* TEM anneals were very non-uniform across the foils, apparently due to thermal conductivity and residual stress issues, so these results were only used as a guide to the temperatures needed for furnace anneals of the thick films. Grain size characterization for the thick films after annealing was done using a scanning electron microscope (SEM) with a backscattered electron detector to enhance grain orientation contrast. Figure 2 shows such an SEM micrograph obtained using 30 keV electrons from a Ni film annealed at 450°C for one hour. The grains are much larger, with an average of 670 nm and standard deviation of 330 nm, comparable to the size of the indentations used for hardness measurements, as shown. An intermediate anneal of 350°C for an hour also enlarged the Ni grain sizes, but only to an average size of 32 nm, near the usable resolution of the SEM, so the estimate of grain sizes may be on the high side for this sample. Further work on the intermediate anneal using cross-section TEM imaging is planned.

INDENTATION TESTING AND FINITE-ELEMENT MODELING

Ultra-low-load indentation testing combined with an analysis based on finite-element modeling was used to evaluate the mechanical properties of the layers.[10] First, work hardening rate and Poisson's ratio for the layers were assumed to be the same as for bulk Ni and Cu. With these parameters set, the analysis then determines the intrinsic yield stress, Young's modulus, and hardness of the layer materials using the indentation data, separating the properties of the thin films from those of the substrate. For each sample a series of 10 indents to 160 nm depth were performed, each with the continuous stiffness measurement (CSM) technique, which uses a small oscillation on the loading force to obtain both indenter force and sample stiffness as a continuous function of depth into the sample.[11] After examining the results to eliminate obviously erroneous data (generally due to hitting surface debris with the indenter), the remaining indent data was averaged and then fit using a finite-element simulation of the experiment. The procedure, described in detail elsewhere [10], involves constructing a mesh which accurately reflects the sample and indenter structure, then fixing the known properties of the substrate and indenter while varying those of the deposited layer (yield stress and elasticity). Once a simulation which gives a good fit to the experimental data is obtained, the deduced yield stress and elasticity for the layer material is used in an additional simulation of an indent into a hypothetical bulk sample of the material in order to obtain a value for the hardness.

Examples of the indent data and the simulation fits for the two Ni samples shown in Figs. 1 and 2 are shown in Fig. 3. Figure 3(a) shows the indent force vs. depth, with the experimental data as circles and squares for the as-deposited Ni and the 450°C anneal, respectively. The best-fit simulations, using $v=0.312$ and a work hardening rate of 0.65 GPa, are shown as solid and dashed lines. Figure 3(b) show the stiffness data and fit. Error bars for the experimental data (generally smaller than the symbols) indicate the standard deviation of the average of the indents. Although the overall sample stiffness changes little with the anneal and larger grain size, the indentation force is dramatically reduced, reflective of a considerable softening of the material.

The properties deduced for as-deposited, fine-grained Ni were:
Young's modulus = 244 ± 14 GPa,

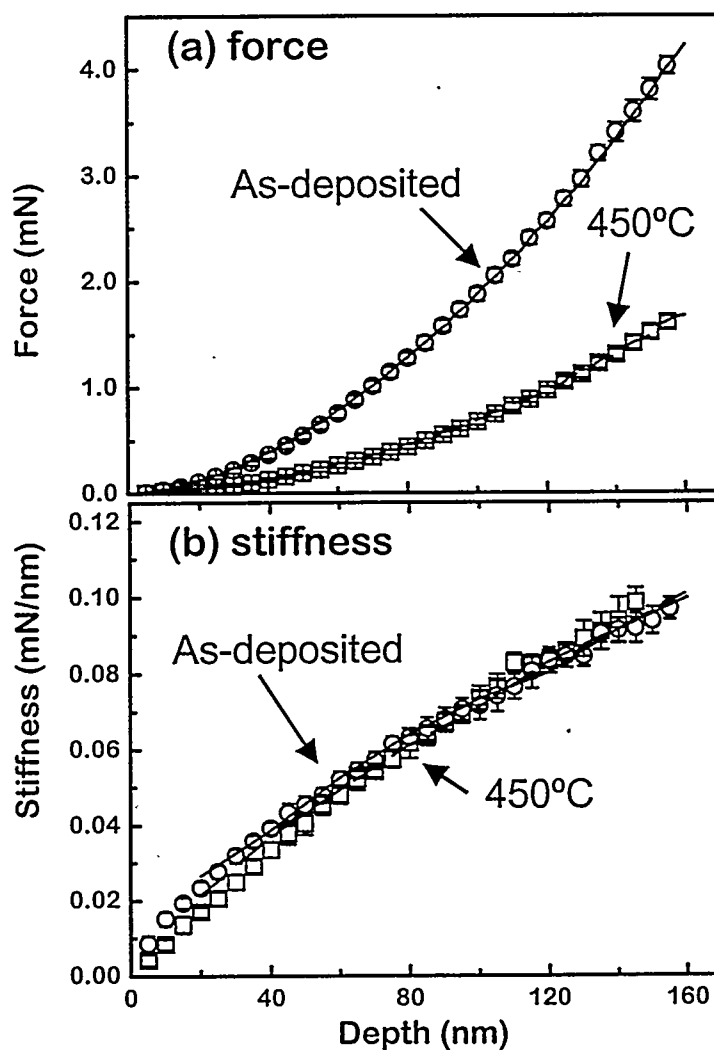


Figure 3. (a) Indentation force and (b) stiffness, data and best-fit simulation, for as-deposited Ni (circles) and Ni annealed to 450°C (squares).

yield stress = 2.52 ± 0.2 GPa, and hardness = 10.3 ± 0.7 GPa. After the 450°C anneal, Young's modulus = 166 ± 15 GPa, yield stress = 0.55 ± 0.1 GPa, and hardness = 2.7 ± 0.4 GPa. The quoted errors include both the spread in experimental data and the accuracy of the simulation fit. The deduced properties may be compared to a Young's modulus of ~ 204 GPa and hardness of ~ 1.1 GPa for bulk Ni.

RESULTS AND DISCUSSION

The comparison of our results to representative earlier work is shown in Figs. 4 and 5, with the hardnesses plotted vs. inverse square root of grain size. The previous Ni data plotted in Fig. 4 is from refs. [3] and [4], both of which studied electrodeposited Ni. Our Ni data are plotted as solid circles, including results for two samples of as-deposited material, the 350 and 450°C anneals, and a large-grained bulk Ni sample examined using the same techniques. For the Cu data in Fig. 5, the previous work is from refs. [5] and [6], using compaction of gas condensation powders and a deformation/annealing technique to refine grain size, respectively. Only one result from our work is shown, for as-deposited PLD Cu.

For both Ni and Cu, our observed hardnesses are higher than found in layers with similar grain sizes made by other techniques, and are consistent with a simple extension Hall-Petch behavior (indicated by the solid line in each figure). The observations suggest that the Hall-Petch relationship may extend to much smaller grain sizes than previously anticipated. An additional inference is that the PLD layers have mechanical properties superior to fine-grain materials prepared by other means, perhaps due to a denser, more uniform microstructure.

ACKNOWLEDGEMENTS

Technical assistance by M. P. Moran, G. Petersen, and K. G. Minor is gratefully acknowledged. Careful indentation measurements by the Nano Instruments Innovation Center of MKS Systems Corp. are appreciated. Sandia is a multiprogram laboratory operated by Sandia

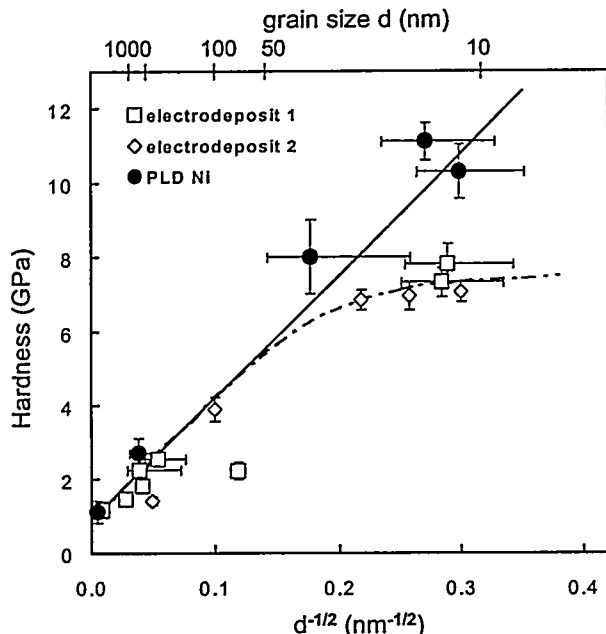


Figure 4. Hardness for Ni as a function of grain size.

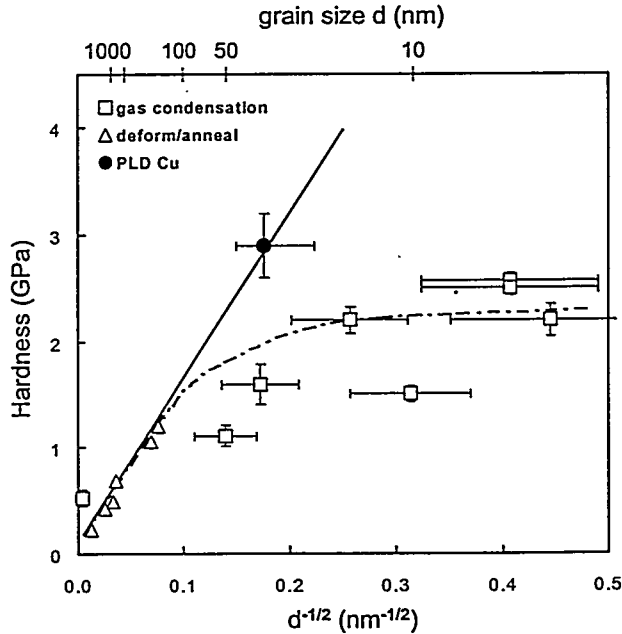


Figure 5. Hardness for Cu as a function of grain size.

Corporation, a Lockheed Martin Company, for the United States Department of Energy under contract DE-AC04-94AL85000. This work was supported by the DOE Office of Basic Energy Sciences.

REFERENCES

1. E. O. Hall, Proc. Phys. Soc. London **B64**, 747 (1951).
2. N. J. Petch, J. Iron Steel Inst. **174**, 25 (1953).
3. G. D. Hughes, S. D. Smith, C. S. Panda, H. R. Johnson, and R. W. Armstrong, Scripta Met. **20**, 93 (1986).
4. A. M. El-Sherik, U. Erb, G. Palumbo, and K. T. Aust, Scripta Met. **27**, 1185 (1992).
5. G. W. Nieman, J. R. Weertman, and R. W. Siegal, J. Mater. Res. **6**, 1012 (1991).
6. R. R. Mulyukov, N. A. Akhmadeev, R. Z. Valiev, and S. B. Mikhailov, Mat. Sci. & Eng. **A171**, 143 (1993).
7. V. G. Gryaznov, M. Yu. Gutkin, A. E. Romanov, and L. I. Trusov, J. Mat. Sci. **28**, 4359 (1993).
8. A. A. Nazarov, Scripta Met. **34**, 697 (1996).
9. C. Suryanarayana and F. H. Froes, Met. Trans. **23A**, 1071 (1992).
10. J. A. Knapp, D. M. Follstaedt, S. M. Myers, J. C. Barbour and T. A. Friedmann, J. App. Phys. **85** (1999) 1460.
11. All of the indentation tests were performed at the Nano Instruments Innovation Center of MTS Systems Corp., Knoxville, TN.